Studies on expression and function of the TMEM16A calcium-activated chloride channel

Fen Huang[a], Jason R. Rock[b,1], Brian D. Harfe[b], Tong Cheng[a], Xiaozhu Huang[c], Yuh Nung Jan[a], and Lily Yeh Jan[a,2]

[a]Howard Hughes Medical Institute and Department of Physiology, University of California, San Francisco, CA 94143; [b]Department of Molecular Genetics and Microbiology, University of Florida, Gainesville, FL 32610; and [c]Lung Biology Center, Department of Medicine, University of California, San Francisco, CA 94158

Calcium-activated chloride channels (CaCC) with similar hallmark features are present in many cell types and mediate important physiological functions including epithelial secretion, sensory signal transduction, and smooth muscle contraction. Having identified TMEM16A of the transmembrane proteins with unknown function (TMEM) 16 family as a CaCC subunit, we have developed antibodies specific for mouse TMEM16A, as evidenced by the absence of immunoreactivity in TMEM16A knockout mice. Here, we show that TMEM16A is located in the apical membranes of epithelial cells in exocrine glands and trachea. In addition, TMEM16A is expressed in airway smooth muscle cells and the smooth muscle cells of reproductive tracts, the oviduct and ductus epididymis. In the gastrointestinal (GI) tract, TMEM16A is absent from smooth muscle cells, but present in the interstitial cells of Cajal (ICC), the pacemaker cells that control smooth muscle contraction. The physiological importance of TMEM16A is underscored by the diminished rhythmic contraction of gastric smooth muscle from TMEM16A knockout mice. The TMEM16A expression pattern established in this study thus provides a roadmap for the analyses of physiological functions of calcium-activated chloride channels that contain TMEM16A subunits.

airway | exocrine gland | interstitial cells of Cajal

The molecular identity of CaCC has been enigmatic for decades (1, 2) and three independent studies using different strategies have recently identified TMEM16A (3–5) and TMEM16B (4) as CaCC subunits. Earlier studies have revealed that, of the 10 members of the mammalian TMEM16 family, TMEM16A expression is up-regulated in gastrointestinal stromal tumors and can serve as a marker for interstitial cells of Cajal (ICC) in the human, primate, and mouse gastrointestinal tract(6), TMEM16E (GDD1) mutation is linked to the human disease *gnathodiaphyseal dysplasia* (7), TMEM16J is a p53-induced gene (8), and TMEM16G is preferentially expressed in normal prostate and prostate cancer cells (9). The molecular identification of TMEM16A and TMEM16B as CaCC subunits has made it possible to examine the physiological functions of calcium-activated chloride channels in molecular and genetic studies.

Recent findings of TMEM16B in photoreceptor terminals (10) and olfactory neuron cilia (11) suggest that calcium-activated chloride channels containing the TMEM16B subunit likely fulfill the negative and positive feedback regulation, respectively, in these sensory neurons. As to TMEM16A, the generation of TMEM16A knockout mice, which fail to thrive and exhibit severe malformation of the tracheal cartilage rings (12), has enabled physiological studies of TMEM16A function in the airway and small intestine (13–15), as well as validation of the TMEM16A antibody specificity. To determine the expression pattern of TMEM16A, we generated rabbit polyclonal antibodies against mouse TMEM16A, revealing that TMEM16A is expressed apically in acinar cells in the pancreas and salivary glands, as well as the airway epithelium.

Interestingly, we found even stronger immunostaining signals in the airway smooth muscle cells (SMCs), another cell type often associated with CaCC function. We therefore examined the TMEM16A expression in several different smooth muscle cells. We found that TMEM16A was also expressed in the smooth muscle cells in the reproductive ducts, oviduct, and ductus epididymis. In the gastrointestinal (GI) tract, however, TMEM16A is expressed not in the smooth muscle cells but in the pacemaker cells, the interstitial cells of cajal (ICCs), as reported in recent studies (6).

In the GI tract, SMC contraction is controlled by the pacemaker cells, the ICCs (16). The pacemaker activity generated by the ICCs induces rhythmic slow waves in the electrically coupled SMCs, thereby controlling the frequency and propagation characteristics of gut contractile activity (16). Pacemaker potentials in the ICCs consist of a transient depolarization followed by a plateau phase with sustained depolarization. The plateau phase is diminished in low $[Cl^-]_o$ solution or solution containing the CaCC inhibitor DIDS, thus implicating the calcium-activated chloride current (17, 18). The high expression of TMEM16A in ICCs raises the possibility that it corresponds to the CaCC implicated for the pacemaker activity that is important for the regulation of smooth muscle contraction. Indeed, we found that the smooth muscle contraction was greatly reduced in the stomach antrum of TMEM16A knockout mice. Our finding that TMEM16A is required for rhythmic contraction of the stomach smooth muscle is further reinforced by a recent report of the absence of slow waves in the small intestine smooth muscle cells from TMEM16A knockout mice (13).

Results

Generation of Polyclonal Antibodies Specific for the Mouse TMEM16A. To determine the expression pattern of TMEM16A, we generated rabbit polyclonal antibodies against the N terminus of mouse TMEM16A, which specifically recognized the TMEM16A-GFP fusion protein expressed in HEK293 cells (Fig. 1A) without exhibiting cross-reactivity against heterologously expressed TMEM16B (Fig. S1). As reported (12), exon12 of the TMEM16A gene is replaced by a vector containing a neomycin resistance gene in TMEM16A knockout mice to terminate the translation by a stop codon supplied by the inserted vector. Our RT-PCR analyses of transcripts in TMEM16A knockout mice revealed the presence of a mutant TMEM16A mRNA without exon12, likely due to alternative splicing (Fig. 1B). This mutant
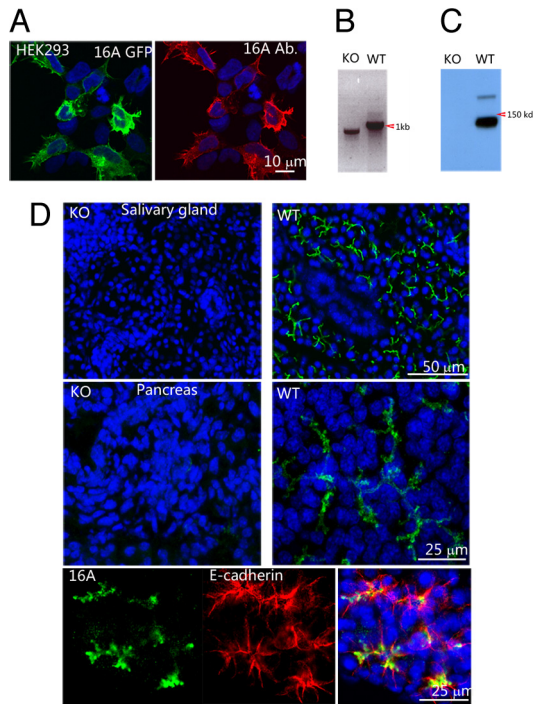
PHYSIOLOGY

www.manaraa.com

Fig. 1. TMEM16A rabbit polyclonal antibody characterization. (*A*) TMEM16A antibody specifically recognizes the TMEM16A-GFP fusion protein exogenously expressed in HEK293 cells. Note the membrane localization of TMEM16A-GFP. (*B*) In TMEM16A wild type mice, the mRNA fragment (995-bp) can be detected by RT-PCR with primers flanking exon12, while a shorter mRNA fragment (838-bp) with exon12 omission can be detected in TMEM16A knockout mouse. (*C*) The mutant TMEM16A-GFP construct does not yield detectable expression of truncated TMEM16A protein in HEK293 cells. (*D*) TMEM16A antibody specifically recognizes the endogenous TMEM16A protein in acinar cells of salivary glands and the pancreas of the wild type mouse. No expression was observed in tissue from the TMEM16A knockout mouse. The *Bottom* reveals the apical localization of TMEM16A in the pancreatic acinar cells by double labeling with the basolateral membrane marker E-cadherin. Blue is the nuclear staining with DAPI.

TMEM16A transcript includes an ORF for a truncated protein containing two transmembrane segments and the same N terminus that should be recognized by the rabbit antibodies we have generated. However, expression of this mutant TMEM16A cDNA without exon12 in HEK293 cells did not give rise to any detectable protein products in Western blots (Fig. 1*C*). Moreover, our antibodies against the TMEM16A N terminus detected no immunoreactivity in vivo (see below), supporting the notion that the TMEM16A knockout mice are null mutants.

CaCC is well known for its function in epithelial secretion (19). Moreover, TMEM16A mRNA has been detected in the salivary gland (3, 4) and siRNA knockdown of TMEM16A reduces the carbachol-induced saliva secretion (3). As shown in Fig. 1*D*, TMEM16A immunoreactivity can be detected in salivary glands from wild type but not TMEM16A knockout mice. Next, we examined the acinar cells in the pancreas, which have apical membranes specialized for secretion. Double labeling with the basolateral membrane maker E-cadherin reveals that TMEM16A is expressed on the apical membranes of the acinar cells in pancreas (Fig. 1*D*). Our findings provide support for a recent study showing the lack of carbachol-induced CaCC in pancreatic acinar cells from TMEM16A knockout mice even though the antibodies used in that study did not detect TMEM16A in the pancreas (14).

TMEM16A Expression in the Airway Epithelial Cells and Smooth Muscle Cells. Airway epithelia use ion transport mechanisms to control the level of airway surface liquid, which is important for mucous
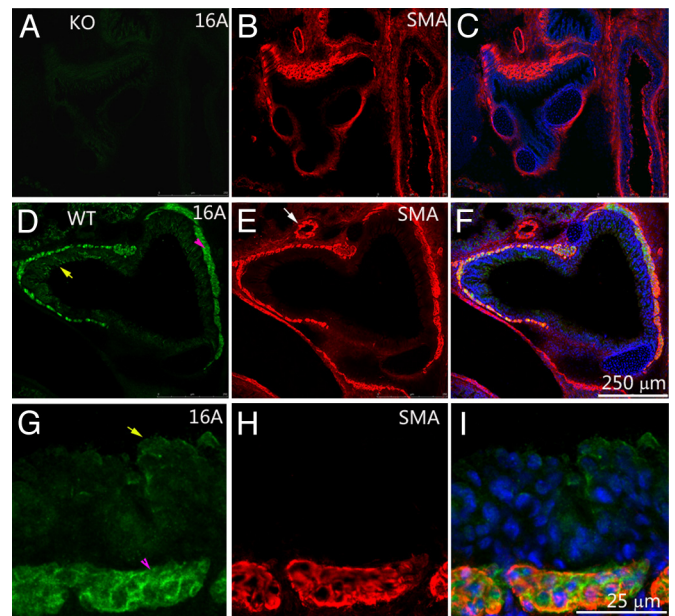

Fig. 2. TMEM16A is expressed in the airway epithelial cells and smooth muscle cells. (*A*) Lack of TMEM16A immunoreactivity in the airway of the TMEM16A knockout mouse. (*B*) Smooth muscle actin (SMA) staining in the airway of the TMEM16A knockout mouse. (*C*) Overlay of *A* and *B*. (*D*) TMEM16A expression in the airway epithelium (yellow arrow) and smooth muscle cells (pink arrowhead) of the wild type mouse. (*E*) SMA staining marks the smooth muscle cells in the wild type airway. (*F*) Overlay of *D* and *E*. (*G*) Higher magnification figure of TMEM16A staining in the wild type airway. (*H*) Higher magnification figure of SMA staining. (*I*) Overlay of *G* and *H*. Note the expression of TMEM16A in the SMA positive SMCs. Blue is the nuclear staining with DAPI.

hydration and removal of irritants and pathogens. Airway epithelial cells have two different chloride channels in their apical membrane, namely the CaCCs and the cystic fibrosis transmembrane regulator (CFTR) (2, 20) and when stimulated with ATP or UTP, they display Ca^{2+} dependent Cl^- secretion (2, 21). Indeed, recent studies have found that tracheas from TMEM16A knockout mice exhibit greatly reduced purinoceptor (UTP)-regulated transepithelial secretion resulting in luminal mucus accumulation (14, 15). Consistent with these physiological studies, we observed TMEM16A in mouse airway epithelial cells, where the TMEM16A protein is concentrated apically (Fig. 2*D* and *G*, yellow arrows).

Interestingly, a higher level of TMEM16A immunoreactivity is present in the smooth muscle layer of the airway (Fig. 2). The TMEM16A protein expression pattern in the airway is in agreement with previous studies (12) showing higher levels of TMEM16A mRNA expression in the tracheal SMCs than epithelium. CaCC has also been implicated in regulating the contraction of vascular smooth muscle; however, there is no detectable signal of TMEM16A immunostaining in the blood vessels in the lung (Fig. 2*E*, white arrow).

TMEM16A Expression in the Reproductive System. In a survey of SMCs in a variety of tissue, we found prominent TMEM16A expression in the smooth muscle cells of the oviduct and ductus epididymis (Fig. 3), but not in the urethra and vas deference (Fig. S2). The oviduct plays an essential role in fertilization for the transport of ova and spermatozoa. The ductus epididymis is the site of sperm maturation, storage, and transport. It will be of interest to explore the potential functional roles of TMEM16A in reproduction in future studies, given that contraction of
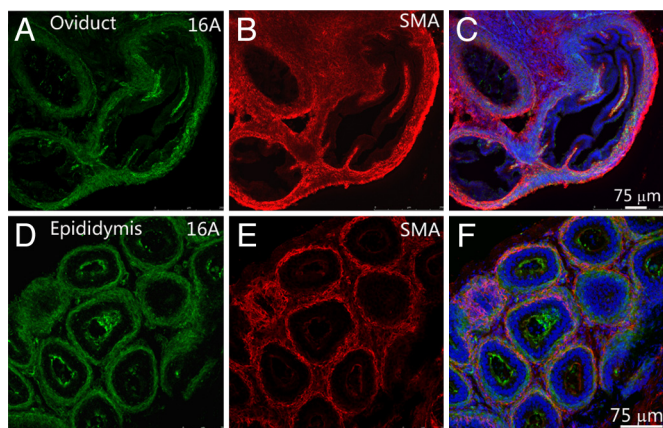
Huang et al.

Fig. 3. TMEM16A is expressed in the SMCs in the reproductive tract. (*A–C*) TMEM16A is expressed in the SMCs of the oviduct. (*D–F*) TMEM16A is expressed in the SMCs of the ductus epididymis. Blue is the nuclear staining with DAPI.

smooth muscle cells of the oviduct and ductus epididymis is important for the propulsion of ovum and spermatozoa (22, 23).

TMEM16A Expression in the Interstitial Cells of Cajal (ICCs) But Not Smooth Muscle Cells in the Gastrointestinal Tract. Unlike some SMCs, which may have endogenous pacemaker activity, smooth muscle contraction in GI tract is controlled by the pacemaker cells, the ICCs (16). Immunostaining with our rabbit polyclonal antibodies yielded strong labeling of ICCs in the stomach and intestine of neonatal wild type mice, while no immunoreactivity could be detected in the TMEM16A knockout mice (Fig. S3). Double staining with the ICC marker C-kit demonstrated that TMEM16A was expressed in the C-kit positive ICCs, but not the smooth muscle actin (SMA) positive SMCs (Fig. 4).

The wall of the GI tract contains two layers of muscles, the inner circular muscle (CM) layer and the outer longitudinal muscle (LM) layer. ICCs display different morphology depending on their location in the GI tract and form gap junctions within ICCs and SMCs (24). For example, multiple processes are elaborated by ICCs in the myenteric plexus (ICC-MY) located between the circular and longitudinal muscle layers and ICCs of submucosa (ICC-SM) at the interface between the submucosal connective tissue and innermost circular muscle layer, whereas ICCs of intramuscular layer (ICC-IM), which are intermingled with smooth muscle bundles in either the circular or the longitudinal layer, are generally spindle shaped with two long and thin processes. We found that TMEM16A was expressed in all types of ICC, including the spindle shaped ICC-IM in the stomach (Fig. 4 *A–C*) and the ICC-SM, ICC-MY and ICC-IM in the intestine (Fig. 4 *D–F*). Three-dimensional surface reconstruction of cells double labeled for TMEM16A and C-kit revealed the multiple processes of ICC-MY and their interconnections forming the ICC network (Fig. 4*J*). Small cellular protrusions with detectable immunoreactivity for TMEM16A but not for C-kit, can also be seen in the 3-D surface reconstruction (Fig. 4*J*).

Defective Smooth Muscle Contraction in the Stomach of TMEM16A Knockout Mice. CaCC has been implicated in generating the slow waves that coordinate rhythmic contraction of the digestive system (17, 18), although other mechanisms remain possible (16, 25, 26). It is therefore important to determine whether the TMEM16A knockout mice display any defect in smooth muscle contraction in the GI tract, the ultimate physiological function of these smooth muscles.

Smooth muscle preparations from the stomach and intestine

exhibit slow waves and maintain rhythmic contractions in vitro (18, 27). Since the slow waves coordinate the smooth muscle contraction, the muscle contraction frequency occurs at the slow wave frequency, for example about three waves per minute in the stomach antrum (27, 28). We have therefore characterized smooth muscle contraction in isolated stomach tissues. Phase contrast images of the stomach antral muscle, pinned on Sylgard with the mucosal side of the circular muscle facing down, were captured in time-lapse (2.5 frames/s).

In the stomach antrum of wild type mice, smooth muscle contraction can be clearly visualized under the microscope as shown in Movies S1 and S2. In contrast to the wild type smooth muscle that contracted in rhythmic broad strokes, smooth muscle contraction in the stomach from TMEM16A knockout mice was reduced in both frequency and amplitude. Individual cells could be resolved in the phase contrast images as they moved along due to the smooth muscle contraction (Fig. S4). By tracking these cells, we estimated the frequency and amplitude of stomach smooth muscle contraction for both wild-type and TMEM16A knockout mice. Such single cell movements reflected the coordinated contraction of circular muscle and longitudinal muscle; the cell position as defined by the coordinates along the circular and longitudinal muscle axis changed in a cyclical pattern. The graph in Fig. 5*A* shows the oscillation of cell position along the axis of the circular muscle orientation for the wild type stomach antral smooth muscle. The frequency of the oscillation is approximately three per minute, which is consistent with the reported slow wave frequency in stomach antrum (27, 28). In contrast, the cell position variation along the circular muscle axis for the TMEM16A knockout mouse stomach antral smooth muscle was less regular, with significantly reduced frequency and amplitude (Fig. 5*B*). When the trajectories of tracked cells are plotted as a function of both coordinates in the circular (*x*) and longitudinal (*y*) muscle axes, clearly, the extent of TMEM16A knockout mouse stomach smooth muscle contraction is severely reduced (Fig. 5*C*). By tracking eight to 10 cells in each SI Movie and measuring the total trajectory length in each case (Fig. 5*D*), we found that the averaged total trajectory length in TMEM16A knockout mice was $\approx 19.881 \pm 0.005\%$ that of wild type control ($P < 0.0001$). Thus, the absence of TMEM16A resulted in greatly reduced stomach smooth muscle contraction.

The observed defect in stomach smooth muscle contraction in TMEM16A knockout mice is likely due to the absence of TMEM16A in ICCs, because both the circular muscle and the longitudinal muscle in the GI tract of TMEM16A knockout mice were organized normally (Fig. S5 *A–D*), and they displayed normal distribution of C-kit positive ICCs (Fig. S5 *E–H*). Thus, the critical role of TMEM16A-mediated CaCC in the generation of slow waves in the small intestine and rhythmic contraction in the stomach reflects an essential function of the CaCC subunit TMEM16A in ICCs as pacemakers in the GI tract.

Discussion

In the present study, we relied on the TMEM16A knockout mice to verify the specificity of antibodies raised against the N terminus of mouse TMEM16A. We show that TMEM16A resides in the apical membrane of airway epithelial cells and acinar cells of the pancreas and salivary glands, the location appropriate for the function of CaCC in regulating secretion. We further show that TMEM16A is also expressed in the airway SMCs. Moreover, we found that TMEM16A is expressed in the SMCs in oviduct and ductus epididymis of the reproductive system, thus raising the possibility of potential involvement of TMEM16A in fertility. Importantly, we found TMEM16A expression in the ICCs but not the SMCs in the GI tract. With the exception of the reproductive tracts, similar TMEM16A expression patterns have been found in adult and neonatal mice. Consistent with previous studies showing that the pacemaker
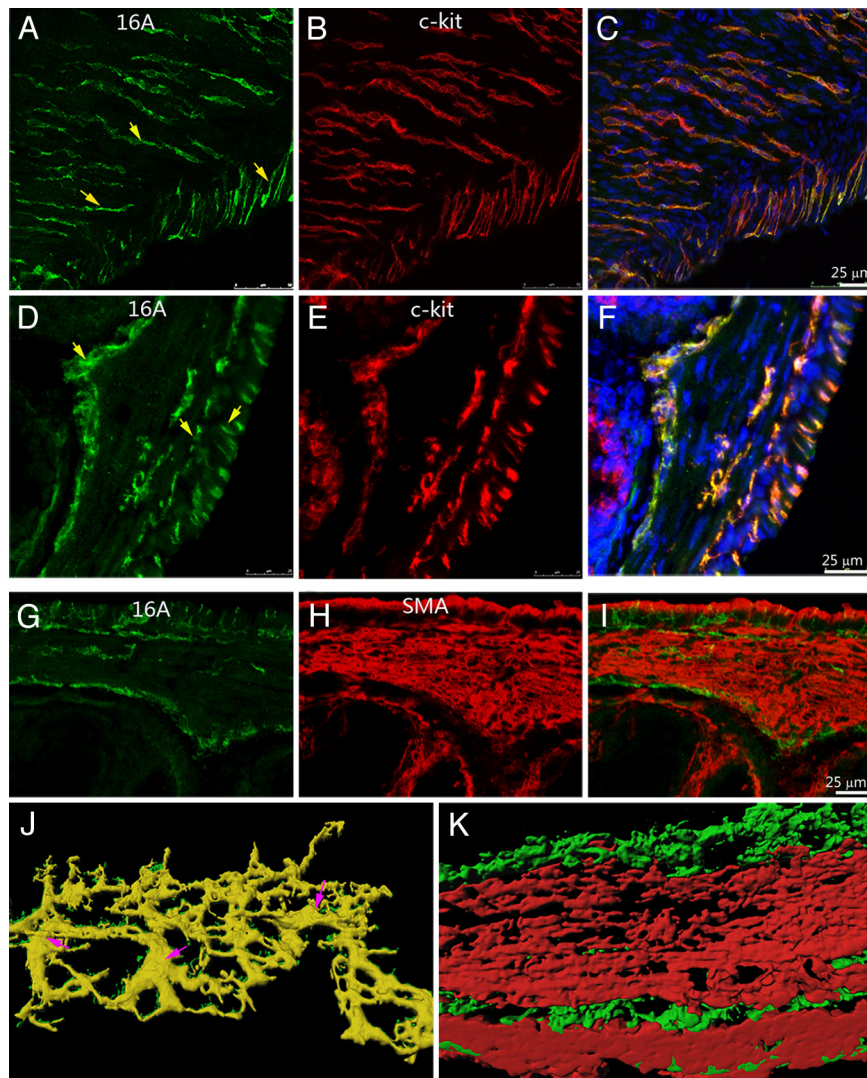
PHYSIOLOGY

Fig. 4. TMEM16A is expressed in the interstitial cells of cajal (ICC) in the mouse stomach and intestine. (*A–C*) TMEM16A is expressed in C-kit positive ICC in the stomach. Arrows point to examples of spindle shaped ICC-IM. (*D–F*) TMEM16A is expressed in C-kit positive ICC in the intestine. Arrows point to examples of ICC-SM, ICC-MY, and ICC-IM. (*G–I*) Double labeling with SMA reveals no detectable expression of TMEM16A in SMCs in the intestine. (*J*) Three-dimensional surface reconstruction of cells double labeled for TMEM16A and C-kit revealed the multiple processes of ICC-MY and their interconnections forming the ICC network. Small cellular protrusions with detectable immunoreactivity for TMEM16A but not for C-kit can also be seen in the 3-D surface reconstruction. Green is TMEM16A and yellow indicates the colocalization of TMEM16A and C-kit. Pink arrows point out the cell bodies of ICC. (*K*) Three-dimensional reconstruction illustrates the spatial relationship of TMEM16A-positive ICC and the SMA-positive SMCs in the intestine. Note the ICC-SM on the top of circular smooth muscle, the ICC-MY between the circular and longitudinal smooth muscle layers and the ICC-IM in the longitudinal muscle layer. Green is TMEM16A and red is SMA. Blue is the nuclear staining with DAPI.

ICCs control SMC contraction, we found that TMEM16A is required for proper smooth muscle contraction in the stomach. Our findings of TMEM16A expression in a variety of tissue provide some indication for common composition of CaCC, and lay the groundwork for future functional studies.

TMEM16A Expression in the Acinar Cells of the Pancreas and Salivary Glands. The salivary glands in mammals are exocrine glands that produce saliva and secrete amylase, an enzyme that breaks down starch for glucose production. The pancreas contains both endocrine glands that release several important hormones such as insulin, glucagon, and somatostatin, and exocrine glands, which secrete digestive enzymes that pass to the small intestine. Both the salivary gland acinar cells and pancreatic acinar cells are polarized epithelial cells with well differentiated basolateral membrane and apical membrane. The transepithelial movement of Cl^- is the primary driving force for fluid and zymogen secretion by exocrine gland acinar cells: the entry of Cl^- across the basolateral membrane is mediated by a $Na^+/K^+/2Cl^-$ co-transporter and the paired Na^+/H^+ and Cl^-/HCO_3^- exchangers, whereas Cl^- exits across the apical membrane via CaCC (19, 29). Indeed, our immunostaining reveals that TMEM16A is localized in the apical membrane of acinar cells, the location appropriate for CaCC function in epithelial secretion.

TMEM16A Is Expressed in the Airway Epithelium and Smooth Muscle Cells. Another cell type well known for its functional requirement of CaCC is the airway epithelial cell. The airway epithelium not only maintains the path for air movement to and from the alveoli, but also plays crucial roles in enabling the lung to remove pathogens and other inhaled particles (30). Several experimental approaches, such as transepithelial short-circuit measurements and whole-cell patch clamp recording, implicate both CaCC and the protein kinase A (PKA)–activated CFTR chloride channel
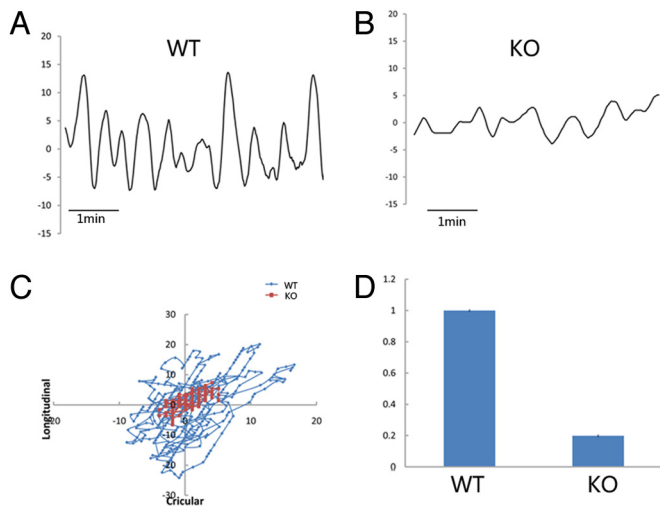
Huang et al.

Fig. 5. Smooth muscle contraction is diminished in the stomach antrum of the TMEM16A knockout mouse. (*A*) Representative cell motility along the axis of the circular muscle orientation for the wild type stomach antral smooth muscle. Note the oscillation of the cell position. (*B*) The cell position variation along the circular muscle axis for the TMEM16A knockout mouse stomach antral smooth muscle is less regular, with significantly reduced frequency and amplitude. (*C*) Representative trajectories of cell movement in the wild type and knockout mouse stomach. The blue trace is wild type and the red is knockout. *X* is the circular muscle axis and *Y* is the longitudinal muscles axis. Note the much larger motility range in the wild type than in the knockout mouse. (*D*) Quantification of the average total trajectory length of cell motility in the wild type and knockout mouse. The average total trajectory length in the knockout is ≈19.88 ± 0.005% of the wild type (n = 8–10 in three pairs of wild type and knockout siblings).

for these important physiological functions of the airway (1, 20, 21). Consistent with physiological studies showing that the TMEM16A knockout mouse trachea exhibits greatly reduced purinoceptor (UTP)-regulated transepithelial transport resulting in luminal mucus accumulation (14, 15), our immunostaining reveals polarized TMEM16A expression in the airway epithelium, where its function is likely to be important in dealing with pulmonary diseases such as cystic fibrosis, chronic bronchitis, and asthma.

Interestingly, in addition to expression in the airway epithelial cells, we found even higher levels of TMEM16A immunoreactivity in the airway smooth muscle cells, an observation of relevance in health and in disease. As to the physiological role of CaCC in airway smooth muscle cell contraction, the airway smooth muscle cells have an endogenous pacemaker mechanism driven by a cytosolic Ca^{2+} oscillator (31). Neurotransmitters and hormones, such as acetylcholine and norepinephrine, induce Ca^{2+} release from internal stores via the inositol trisphospate receptor and the ryanodine receptor. The elevation of cytosolic Ca^{2+} can activate CaCC, thereby causing membrane depolarization and further calcium influx through the voltage-gated calcium channels (32, 33). Moreover, Ca^{2+} sparks in airway SMCs may trigger spontaneous transient inward current (STIC) by opening CaCC (31, 34). Airway smooth muscle also plays a multifaceted role in the pathogenesis of asthma. Not only is excessive contraction of airway smooth muscle a major cause of airway narrowing in asthma, both airway hyperresponsiveness and excess smooth muscle mass have been found in patients with fatal asthma (35). Given the importance of SMCs in the pathology of asthma, TMEM16A expression in the airway smooth muscle has important therapeutic implications.

TMEM16A Is Expressed in SMCs of the Reproductive Tract. In the reproductive system, passage of spermatozoa through the epi-

didymis, which is obligatory for sperm maturation, relies on spontaneous phasic contractions of the ductus epididymis. Similarly, transport of ovum from the ovary to the uterus and transport of spermatozoa to the oviduct may be aided by muscular contractions in the wall of the oviduct. Electrical slow waves have been recorded in the mouse smooth muscle of the reproductive tract (23, 36, 37), although studies thus far are less extensive compared to studies of the GI tract. The smooth muscle activity in reproductive ducts is subject to regulation by adrenergic nerves, sex steroids, nitric oxide, and prostaglandins (PGs). For example, prostaglandin F2 alpha (PGF2α) results in an increase in oviduct muscular contractility (37). PGF2α stimulates the phospholipase C (PLC)-IP$_3$ pathway and Ca^{2+} mobilization, which can activate CaCC to cause membrane depolarization and voltage-gated calcium channel activation (31). The presence of TMEM16A in both the ductus epididymis in the male and the oviduct in the female raises the question whether CaCC contributes to smooth muscle contractility in the reproductive tract; studies of conditional knockout mice will be necessary for the examination of the physiological role of TMEM16A-mediated CaCC in fertility.

TMEM16A in the Pacemaker ICC of the GI Tract Is Critically Involved in the Control of Smooth Muscle Contraction. Contractions of the SMCs in the gastrointestinal (GI) tract serve two basic functions, grinding and mixing the ingested food and propelling the food along the length of the GI tract (28, 38). Slow waves organize the phasic contractions of GI muscles to mediate gastric peristalsis and intestinal segmentation. GI SMCs are not capable of generating slow wave by themselves; instead ICCs are the pacemakers, which are electrically coupled to the SMCs (16, 38). Whereas a number of different ion channels may be involved in the generation of slow waves (16–18, 25, 26, 39), one attractive hypothesis is that the initiation of slow wave is caused by the release of Ca^{2+} from internal stores via IP$_3$ receptor, leading to the spontaneous transient inward current (STIC) (31). Summation of STIC results in the spontaneous transient depolarization (STD) in the ICCs that initiates the slow wave. Calcium-activated chloride channels have been implicated for the STIC and also the plateau phase of depolarization in the slow wave (17, 18, 31, 38). The expression of TMEM16A in ICCs documented by us and by others (6, 13), provides the molecular evidence for CaCC in ICC. The requirement of TMEM16A for stomach smooth muscle contraction reported here, together with a similar requirement of TMEM16A for generating slow waves in small intestine smooth muscle (13), underscores the physiological importance of CaCC for GI rhythmic contraction.

In summary, in addition to finding TMEM16A at the apical membrane for epithelial and exocrine secretion, we have found TMEM16A expression in the SMCs of the airway and the oviduct and ductus epididymis of the reproductive tract, as well as the ICC pacemaker cells in the GI tract. One common feature of these different cell types is that their calcium signaling is driven by elevation of the cytosolic Ca^{2+} level, which may exhibit oscillations due to periodic release via IP$_3$ receptors (31). TMEM16A might serve as the downstream effector of calcium release from internal stores, as well as calcium influx, and cause depolarization leading to further calcium influx and activation of voltage-gated ion channels (40); such positive feedback regulation is likely to be crucial for smooth muscle functions in a wide range of tissues.

Methods

TMEM16A Antibody Generation. The rabbit polyclonal antibody for TMEM16A was raised against the N terminus of mouse TMEM16A (RVPEKYSTLPAEDR) and used for immunocytochemical staining of wild type and TMEM16A knockout mice (details of the knockout mice generation have been reported in ref. 12.

Time Lapse Imaging of Smooth Muscle Contraction. For measurement of smooth muscle contraction of stomach from postnatal day 3 (P3) TMEM16A knockout and wild type siblings, the antral portion of stomach was cut and opened along the lesser curvature. The mucosal layer was removed by sharp dissection. The antral muscle preparation with intact circular and longitudinal muscle layers was pinned on Sylgard at the bottom of a recording chamber with the mucosal side of the circular muscle facing down. Muscles were maintained 31.4 ± 0.2 °C in KRB buffer (pH 7.3–7. 4) containing (in mM): Na^+, 137.4; K^+, 5.9; Ca^{2+}, 2.5; Mg^{2+}, 1.2; Cl^-, 134; HCO_3^-, 15.5; $H_2PO_4^-$, 1.2; dextrose, 11.5; and bubbled with 95% O_2-5% CO_2. The smooth muscles were equilibrated in the KRB buffer for 1 h before imaging. Phase-contrast time-lapse images, focused at the level of the longitudinal muscle layer, were recorded using MetaVue (Molecular Devices) with a 60× water-immersion objective lens at 2.5 frames per s, stored in TIF stacks of several hundred frames, and analyzed by ImageJ.

Image Analysis and Data Processing. The cell movement in the time lapse images was manually tracked with ImageJ. The x and y coordinates of the cell position were generated by clicking on the tracked cell in sequential images. Datasets of x and y coordinates of the tracked cells were exported to Excel. Since the axes of circular muscle and longitudinal muscle run perpendicular to each other, and the longitudinal muscle axis can be distinguished in the phase-contrast image, we obtained the cell position coordinates in the circular and longitudinal muscle axes by rotating the x and y axes accordingly. Specifically, the angle of longitudinal muscle axis with the x axis was measured by ImageJ as θ, and then new coordinates were calculated as: $x' = x\cos(\theta) + y\sin(\theta)$ and $y' = -x\sin(\theta) + y\cos(\theta)$. The original coordinates are x and y, and x' and y' are the new coordinates aligned with the circular muscle and longitudinal muscle axes. The relative position changes, which were calculated by subtracting the average of x' or y' values from the absolute position coordinates x' and y', were plotted over time, as shown in Fig. 5 A and B.

Similarly, the trajectory of cell movement is plotted in the circular and longitudinal muscle axes with the new coordinates, x' and y', as shown in Fig. 5C. The total trajectory length of each tracked cell was calculated as the sum of a sequence of ''n'' straight-line segments, each corresponding to the cell translocation in a given time interval. The average total trajectory length of all of the tracked cells in the TMEM16A knockout mouse tissue was normalized to that of their wild type siblings and the average percentage is obtained from all of the paired experiments. See *SI Text* for further details.

1. Eggermont J (2004) Calcium-activated chloride channels: (Un)known, (un)loved? *Proc Am Thorac Soc* 1:22–27.
2. Hartzell C, Putzier I, Arreola J (2005) Calcium-activated chloride channels. *Annu Rev Physiol* 67:719–758.
3. Yang YD, et al. (2008) TMEM16A confers receptor-activated calcium-dependent chloride conductance. *Nature* 455:1210–1215.
4. Schroeder BC, Cheng T, Jan YN, Jan LY (2008) Expression cloning of TMEM16A as a calcium-activated chloride channel subunit. *Cell* 134:1019–1029.
5. Caputo A, et al. (2008) TMEM16A, a membrane protein associated with calcium-dependent chloride channel activity. *Science* 322:590–594.
6. Gomez-Pinilla PJ, et al. (2009) Ano1 is a selective marker of interstitial cells of Cajal in the human and mouse gastrointestinal tract. *Am J Physiol Gastrointest Liver Physiol* 296:G1370–G1381.
7. Tsutsumi S, et al. (2005) Molecular cloning and characterization of the murine gnathodiaphyseal dysplasia gene GDD1. *Biochem Biophys Res Commun* 331:1099–1106.
8. Polyak K, Xia Y, Zweier JL, Kinzler KW, Vogelstein B (1997) A model for p53-induced apoptosis. *Nature* 389:300–305.
9. Das S, et al. (2008) Topology of NGEP, a prostate-specific cell: Cell junction protein widely expressed in many cancers of different grade level. *Cancer Res* 68:6306–6312.
10. Stohr H, et al. (2009) TMEM16B, a novel protein with calcium-dependent chloride channel activity, associates with a presynaptic protein complex in photoreceptor terminals. *J Neurosci* 29:6809–6818.
11. Stephan AB, et al. (2009) ANO2 is the cilial calcium-activated chloride channel that may mediate olfactory amplification. *Proc Natl Acad Sci USA* 106:11776–11781.
12. Rock JR, Futtner CR, Harfe BD (2008) The transmembrane protein TMEM16A is required for normal development of the murine trachea. *Dev Biol* 321:141–149.
13. Hwang SJ, et al. (2009) Expression of anoctamin 1/TMEM16A by interstitial cells of Cajal is fundamental for slow wave activity in gastrointestinal muscles. *J Physiol* 587:4887–4904.
14. Ousingsawat J, et al. (2009) Loss of TMEM16A causes a defect in epithelial Ca^{2+} dependent chloride transport. *J Biol Chem* 284:28698–28703.
15. Rock JR, et al. (2009) Transmembrane protein 16A (TMEM16A) is a Ca^{2+}-regulated Cl^- secretory channel in mouse airways. *J Biol Chem* 284:14875–14880.
16. Sanders KM, Koh SD, Ward SM (2006) Interstitial cells of cajal as pacemakers in the gastrointestinal tract. *Annu Rev Physiol* 68:307–343.
17. Hirst GD, Bramich NJ, Teramoto N, Suzuki H, Edwards FR (2002) Regenerative component of slow waves in the guinea-pig gastric antrum involves a delayed increase in $[Ca^{2+}]_i$ and Cl^- channels. *J Physiol* 540:907–919.
18. Kito Y, Suzuki H (2003) Properties of pacemaker potentials recorded from myenteric interstitial cells of Cajal distributed in the mouse small intestine. *J Physiol* 553:803–818.
19. Melvin JE, Yule D, Shuttleworth T, Begenisich T (2005) Regulation of fluid and electrolyte secretion in salivary gland acinar cells. *Annu Rev Physiol* 67:445–469.
20. Anderson MP, Sheppard DN, Berger HA, Welsh MJ (1992) Chloride channels in the apical membrane of normal and cystic fibrosis airway and intestinal epithelia. *Am J Physiol* 263:L1–L14.
21. Boucher RC, et al. (1989) Chloride secretory response of cystic fibrosis human airway epithelia. Preservation of calcium but not protein kinase C- and A-dependent mechanisms. *J Clin Invest* 84:1424–1431.
22. Kunikata K, Yamano S, Tokumura A, Aono T (1999) Effect of lysophosphatidic acid on the ovum transport in mouse oviducts. *Life Sci* 65:833–840.
23. Mewe M, Bauer CK, Muller D, Middendorff R (2006) Regulation of spontaneous contractile activity in the bovine epididymal duct by cyclic guanosine 5'-monophosphate-dependent pathways. *Endocrinology* 147:2051–2062.
24. Komuro T (2006) Structure and organization of interstitial cells of Cajal in the gastrointestinal tract. *J Physiol* 576:653–658.
25. Parsons SP, Sanders KM (2008) An outwardly rectifying and deactivating chloride channel expressed by interstitial cells of cajal from the murine small intestine. *J Membr Biol* 221:123–132.
26. Zhu Y, Mucci A, Huizinga JD (2005) Inwardly rectifying chloride channel activity in intestinal pacemaker cells. *Am J Physiol Gastrointest Liver Physiol* 288:G809–G821.
27. Hirst GD, Garcia-Londono AP, Edwards FR (2006) Propagation of slow waves in the guinea-pig gastric antrum. *J Physiol* 571:165–177.
28. Hirst GD, Edwards FR (2006) Electrical events underlying organized myogenic contractions of the guinea pig stomach. *J Physiol* 576:659–665.
29. Thevenod F (2002) Ion channels in secretory granules of the pancreas and their role in exocytosis and release of secretory proteins. *Am J Physiol Cell Physiol* 283:C651–C672.
30. Crystal RG, Randell SH, Engelhardt F, Voynow J, Sunday ME (2008) Airway epithelial cells: Current concepts and challenges. *Proc Am Thorac Soc* 5:772–777.
31. Berridge MJ (2008) Smooth muscle cell calcium activation mechanisms. *J Physiol* 586:5047–5061.
32. Liu X, Farley JM (1996) Acetylcholine-induced Ca^{2+}-dependent chloride current oscillations are mediated by inositol 1,4,5-trisphosphate in tracheal myocytes. *J Pharmacol Exp Ther* 277:796–804.
33. Kotlikoff MI, Wang YX (1998) Calcium release and calcium-activated chloride channels in airway smooth muscle cells. *Am J Respir Crit Care Med* 158:S109–S114.
34. Bao R, et al. (2008) A close association of RyRs with highly dense clusters of Ca^{2+}-activated Cl^- channels underlies the activation of STICs by Ca^{2+} sparks in mouse airway smooth muscle. *J Gen Physiol* 132:145–160.
35. Hershenson MB, Brown M, Camoretti-Mercado B, Solway J (2008) Airway smooth muscle in asthma. *Annu Rev Pathol* 3:523–555.
36. Talo A, Hodgson BJ (1978) Electrical slow waves in oviductal smooth muscle of the guinea-pig, mouse and the immature baboon. *Experientia* 34:198–200.
37. Sinback CN, Shain W (1979) Electrophysiological properties of human oviduct smooth muscle cells in dissociated cell culture. *J Cell Physiol* 98:377–393.
38. Suzuki H (2000) Cellular mechanisms of myogenic activity in gastric smooth muscle. *Jpn J Physiol* 50:289–301.
39. Park SJ, McKay CM, Zhu Y, Huizinga JD (2005) Volume-activated chloride currents in interstitial cells of Cajal. *Am J Physiol Gastrointest Liver Physiol* 289:G791–G797.
40. Leblanc N, et al. (2005) Regulation of calcium-activated chloride channels in smooth muscle cells: A complex picture is emerging. *Can J Physiol Pharmacol* 83:541–556.

Huang et al.

www.manaraa.com